Magnetic Resonance Materials in Physics, Biology and Medicine (2019) 32:205–212
https://doi.org/10.1007/s10334-018-0704-x

RESEARCH ARTICLE

Characterization of a clinically used charcoal suspension for in vivo EPR oximetry

Céline Marie Desmet[1] · Ly Binh An Tran[1] · Pierre Danhier[1] · Bernard Gallez[1]

Received: 30 May 2018 / Revised: 21 August 2018 / Accepted: 31 August 2018 / Published online: 12 September 2018

Abstract

Objectives Electron paramagnetic resonance (EPR) oximetry using particulate materials allows repeatable measurements of oxygen in tissues. However, the materials identified so far are not medical devices, thus precluding their immediate use in clinical studies. The aim of this study was to assess the magnetic properties of Carbo-Rep®, a charcoal suspension used as a liquid marker for preoperative tumor localization.

Materials and methods Calibration curves (EPR linewidth as a function of pO_2) were built using 9-GHz EPR spectrometry. The feasibility of performing oxygen measurements was examined in vivo by using a low-frequency (1 GHz) EPR spectrometer and by inducing ischemia in the gastrocnemius muscle of mice or by submitting rats bearing tumors to different oxygen-breathing challenges.

Results Paramagnetic centers presenting a high oxygen sensitivity were identified in Carbo-Rep®. At 1 GHz, the EPR linewidth varied from 98 to 426 µT in L-band in nitrogen and air, respectively. The sensor allowed repeated measurements of oxygen over 6 months in muscles of mice. Subtle variations of tumor oxygenation were monitored in rats when switching gas breathing from air to carbogen.

Discussion The magnetic properties of Carbo-Rep® are promising for its future use as oxygen sensor in clinical EPR oximetry.

Keywords EPR · ESR · Oximetry · Charcoal · Tumor hypoxia

Introduction

Oxygen is a critical factor in physiology, pathophysiology, and therapy. In many circumstances, the ability to measure oxygenation is critical to assess tissue function and disease. Several potentially useful methods are able to measure tissue oxygen level [1–3]. These methods are based on the accumulation of nitroimidazoles in hypoxic cells evidenced by immunohistochemistry [4] or positron emission tomography (PET) [5], fluorescence and phosphorescence quenching [6], electrochemical reaction [7], and magnetic resonance (MR) techniques. Oxygen-sensitive MRI techniques include T_2* and T_1 measurements [8–13], as well as fluorine relaxometry [14, 15], as illustrative examples. Electron paramagnetic resonance (EPR) offers the possibility of providing quantitative pO_2 values using paramagnetic centers sensitive to the oxygen environment [16–20]. Among the potential EPR oxygen sensors, particulate materials offer several advantages: they are highly sensitive to variations of oxygen (changes <1 mmHg can be detected), and they are inert in tissues, leading to the possibility of repeat oxygen measurements from the same site over long periods (months to years) [16, 17, 19]. Several particulate materials have been identified for that purpose: lithium phthalocyanine [21] and substituted lithium naphthalocyanine [22], charcoals [23], and carbon blacks [24]. These particulate sensors were successfully used in preclinical studies to measure oxygen in brain [25], heart [26], skeletal muscle [27], liver [28], gastrointestinal tract [29], kidney [30], skin [31], ovarian grafts [32], pancreatic islet grafts [33], and wounds [34]. One of the largest successes of EPR oximetry has been the monitoring of variations in tumor oxygenation induced by pharmacological agents [35–41] or during the course of radiation therapy [42–45].

C. M. Desmet and L. B. A. Tran contributed equally to the study.

✉ Bernard Gallez
Bernard.Gallez@uclouvain.be

[1] Biomedical Magnetic Resonance Research Group, Louvain Drug Research Institute, Université catholique de Louvain, Avenue Mounier 73-B1.73.08, 1200 Brussels, Belgium

The development of advanced whole-body low-frequency EPR systems [46] has opened up the possibility of translating this unique technology to measure tissue oxygenation in patients [47, 48]. When moving into the clinical arena, the most crucial issue is to ensure the biocompatibility of the oxygen sensors [49]. The seminal idea was to use India ink [50], which contains carbon-black particles, as this material has been used for several centuries for tattooing humans. However, as the paramagnetic properties largely varied from batch to batch, synthetic biocompatible India inks were developed using well-characterized carbon-black materials [24] and suspended in pharmaceutical-grade suspending agents [51]. Besides the use of inks, many efforts focused on the inclusion of paramagnetic sensors in thin oxygen-permeable biocompatible materials [52–58]. Still, researchers with an interest in applying EPR oximetry in patients are facing regulatory problems, namely, the need for production of experimental oxygen sensors according to good manufacturing practice (GMP) standards and the potential request for approval as an authorized medical device. These regulatory issues encouraged us to screen the EPR properties and oxygen sensitivity of carbon materials already approved as medical devices. From this screening, we identified Carbo-Rep® as a promising candidate for the application of EPR oximetry in patients. Carbo-Rep® is a sterile suspension of charcoal that is used in Europe for the accurate preoperative localization of mammographically detected lesions. This charcoal suspension is approved as a medical device class IIb. In this publication, we described the EPR characteristics of this charcoal with a focus on its sensitivity to oxygen. In addition, we performed in vivo experiments in mice and rats using low-frequency EPR to assess its ability to identify subtle variations of oxygenation in muscle and tumors and its long-term responsiveness as an oxygen sensor.

Materials and methods

Chemicals

Carbo-Rep® (40 mg charcoal/ml) was purchased from Sterylab (Milan, Italy). The suspension was shaken before sampling. All measurements were carried out on the suspension as received without any additional chemicals. The following batches were analyzed: nos. 0613-17 and 1152-17.

Particle size

The particle size and the polydispersity index (PDI) were characterized by dynamic light scattering (DLS) using a Zetasizer Nano ZS (Malvern Instruments Ltd., Worcestershire, UK).

In vitro 9-GHz EPR spectrometry

EPR measurements were performed using a Bruker EMX-Plus spectrometer (Bruker, Rheinstetten, Germany) operating at X-band (9.4 GHz) and equipped with a PremiumX ultra-low-noise microwave bridge and a Super High Q (SHQ) high-sensitivity resonator. EPR settings were as follows: microwave power 1.262 mW; modulation frequency 100 kHz; modulation amplitude 0.02 mT; time constant 10.24 ms; conversion time 15 ms; data points 3000; sweep width 3 mT. Calibration curves of linewidth (LW) as a function of pO_2 were done at 296 and 310 K. Approximately 50µl of charcoal suspension were placed in a gas-permeable Teflon tube (inner diameter 0.025 in.; outer diameter 0.029 in.; Zeus Industrial Products, Letterkenny, Ireland). The Teflon tube was inserted in a quartz tube open at both ends. The oxygen content was varied between 0 and 21% O_2 using an Aalborg gas mixer. The oxygen content in the mixed gas was measured using a Servomex MiniMP 5200 oxygen analyzer (precision 0.1% oxygen content). The gas flux in the EPR cavity was 270 l/h.

In vitro 1-GHz EPR spectrometry

The oxygen calibration curve at 310 K was also performed on a low-frequency EPR spectrometer (Clin-EPR LLC, Lyme, NH, USA) equipped with a loop-gap surface coil. Approximately 500µl of charcoal suspension was placed in a glass vial, which was placed in a water bath at 310 K. A gas with oxygen content varying between 0 and 21% O_2 was flushed for 75 min in the suspension through a needle. A second needle, inserted in the plug, was used to avoid hyperpressure in the vial. The oxygen content in the mixed gas was measured by a Servomex MiniMP 5200 oxygen analyzer. Needles were removed and vials placed on the loop-gap surface coil. EPR measurements were performed immediately.

In vivo 1-GHz EPR spectrometry

Anesthesia

Animals were anesthetized by inhalation of isoflurane mixed with air (21% oxygen) in a continuous flow (2 l/h) delivered by a nose cone. Induction of anesthesia was performed using 3% isoflurane which was then stabilized at 1.5% for a minimum of 15 min before any measurement. It was previously demonstrated that this anesthesia regimen did not disturb the

hemodynamics in rodents [59]. A circulating water system was used for body-temperature regulation at 37 °C.

Muscle

Male C57BL/6 mice (Janvier, Le Genest-Saint-Isle, France) ($n=5$) were used for the studies in muscle; 75 µl of charcoal suspension was injected in both gastrocnemius muscles. The first EPR measurement was done 1 day after administration of the oxygen sensor. Measurements were repeated over 6 months. In vivo measurements were performed using a low-frequency EPR spectrometer (Clin-EPR LLC) equipped with a loop-gap surface coil. In two of five experimental animals, measurements were carried out on muscles before and after transient restriction of the blood supply (the base of the thigh was reversibly tied for 5 min with a thread to restrict flow through the femoral arteries). In total, ten muscles were measured at the basal state at each time point over 6 months and four muscles during transient ischemic periods.

Tumors

Seven-week-old male Fischer 344 rats (Charles River, Arbresle, France) ($n=3$) were subcutaneously injected with 5.10^6 9L-glioma cells (kindly provided by Dr. Olivier Bockstael, Université Libre de Bruxelles, Belgium) in the thigh. Tumor implantation was performed under anesthesia with a mixed solution of ketamine and xylazine at doses of 80 and 10 mg/kg, respectively. Rats were included in the study when the tumor reached a diameter of 14–16 mm. Approximately 400µl of charcoal suspension was introduced within the tumor at a depth of 3–6 mm. EPR acquisitions were first carried out at 1 day after probe implantation. After recording the pO_2 value under normoxic condition, the input gas was switched from air to carbogen (5% CO_2 in oxygen). The pO_2 value under hyperoxic condition was obtained after 30-min carbogen breathing. The experiment was repeated the following day (2 days after probe implantation) with the same animals.

Results

The Carbo-Rep® preparation is a suspension of charcoal particles with a small diameter (mean 2.9 µm, PDI = 0.55), allowing easy sampling for injection. This charcoal suspension presents an EPR spectrum characteristic of a carbon-centered radical (Fig. 1) with a g-value of 2.00315. The microwave-power saturation curve is presented in Fig. 1. Interestingly, the EPR LW was highly sensitive to the oxygen environment, as shown in Fig. 1. The calibration curves (LW as a function of % oxygen) recorded in X-Band and L-Band are presented in Fig. 2. This calibration was

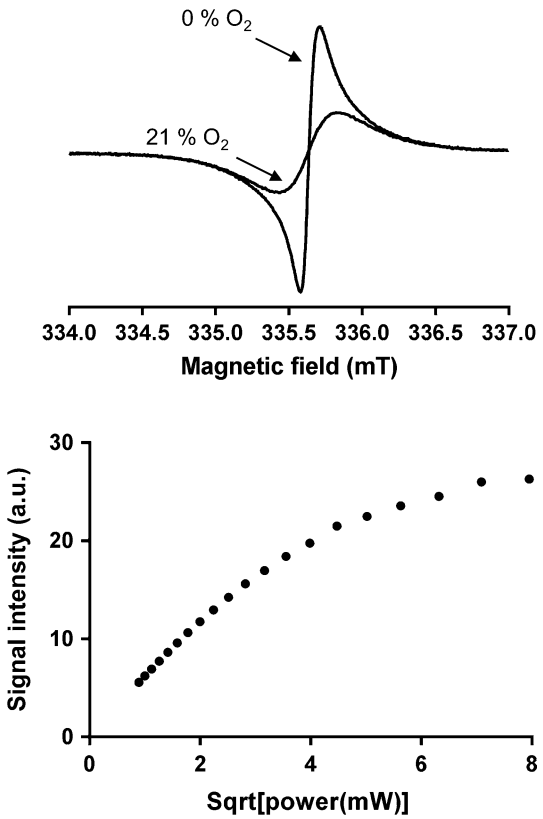

Fig. 1 Electron paramagnetic resonance (EPR) characteristics of the charcoal suspension present in Carbo-Rep®. Top: EPR spectra recorded at 9 GHz in air and in nitrogen. Bottom: microwave-power saturation curve

reproducible from vial to vial and from batch to batch (Fig. 2 top). We found that the calibration was slightly dependent on the temperature (Fig. 2 middle). In L band (Fig. 2 bottom), we observed a slightly different calibration compared to X band, particularly <2% O_2, where LW was lower for the same O_2 percentage. Low-frequency (1 GHz) EPR spectrometry was used to assess the performance of Carbo-Rep® as an oxygen sensor in vivo. Figure 3 presents a typical EPR spectrum recorded in vivo in the muscle after administration of 75µl of charcoal suspension. The LW varied considerably when the blood flow was temporarily interrupted in the muscle (Fig. 3). We repeated the measurements of the LW over a period of 6 months, which showed that Carbo-Rep® preserved its responsiveness to variations in oxygenation in vivo (Fig. 4). Mean pO_2 values are presented in Fig. 4. As expected, the administration of Carbo-Rep® induced no inflammatory response or damage in the muscle injected (Fig. 5). Carbo-Rep® was also administered in a glioma tumor model. The charcoal was distributed over the whole tumor, allowing measurement of the pO_2 distributed in the whole tumor (Fig. 6). Baseline pO_2 values (while rats were breathing air) indicated that these tumors were highly

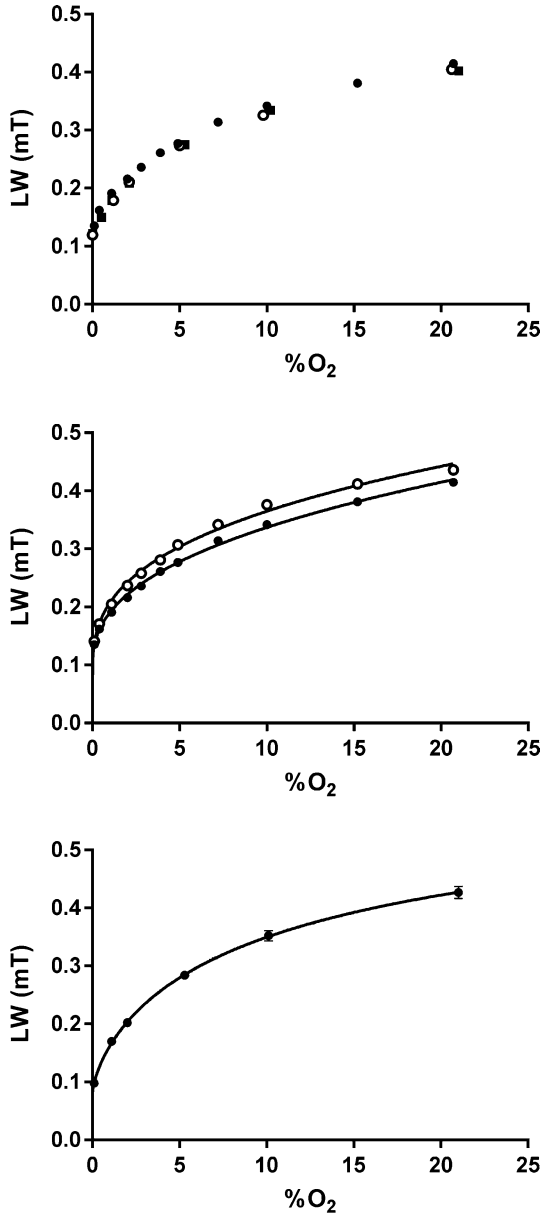

Fig. 2 Calibration curves [linewidth (LW) as a function of percent O_2] of charcoal suspension present in Carbo-Rep®. Top: oxygen calibrations carried out on three different flasks in X band. Closed circle: batch no. 0613-17 vial 1; Open circle: batch no. 0613-17 vial 2; Closed square: batch no. 1152-17 vial 1. Middle: effect of temperature on oxygen calibration in X band. Open circle: 296 K. Closed circle: 310 K. Bottom: oxygen calibration performed in L band (1 GHz). Results are expressed as mean ± standard deviation (SD) ($n=4$)

hypoxic (Fig. 7). Individual tumor responses to a carbogen-breathing challenge are also presented. There was a large heterogeneity in response to carbogen breathing: the pO_2 reached values >10 mmHg in three of six tumors. Overall, the increase in pO_2 was significant.

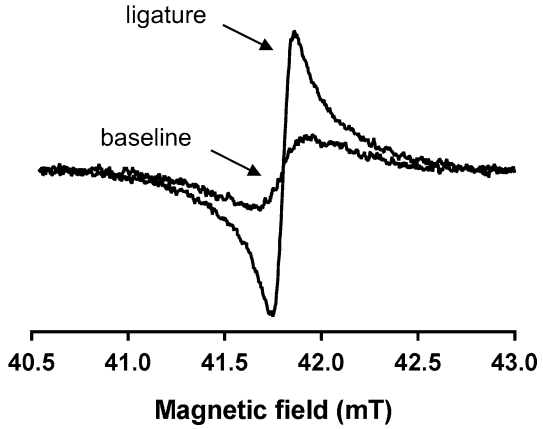

Fig. 3 Typical electron paramagnetic resonance (EPR) spectra recorded in vivo using a 1-GHz EPR spectrometer in the gastrocnemius muscle of a mouse before and after transient restriction of the blood flow

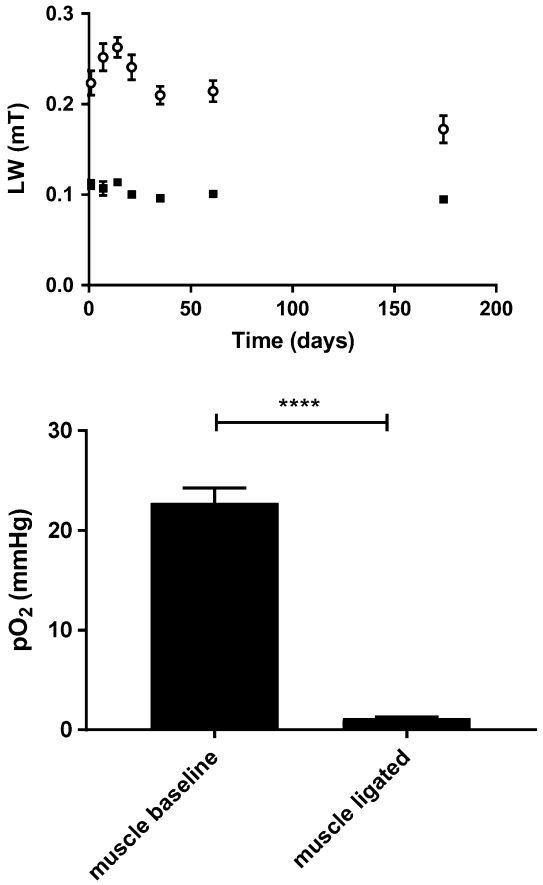

Fig. 4 Measurements of line width (LW) and pO_2 estimates recorded in vivo in the muscle of mice after administration of Carbo-Rep®. Top: electron paramagnetic resonance (EPR) LW measured over time in normal muscles ($n=10$, open circle) and hypoxic muscles ($n=4$, closed square). Bottom: mean pO_2 values ± standard error of mean (SEM) measured in muscles and hypoxic muscles. ****$P<0.0001$

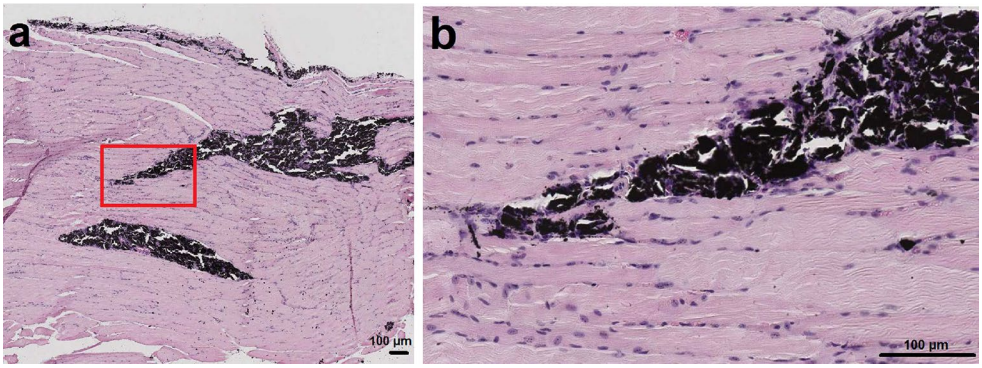

Fig. 5 Histological section in a muscle injected with Carbo-Rep® (**a**) and magnification of area close to sensor location (**b**). Minimal inflammation, if any, was observed around the charcoal material

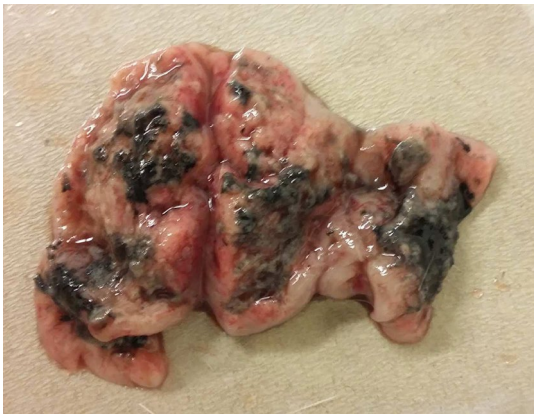

Fig. 6 Distribution of the charcoal inside a tumor

Discussion

While tissue oxygenation is critical in the management of many pathologies, current clinical practice often uses indirect markers of tissue hemodynamics. However, there are several circumstances in which the knowledge of real pO_2 values could potentially impact the clinical decision. The most obvious field is radiation therapy, as the response to irradiation is dramatically dependent on pO_2 values in the range of 0–10 mmHg [60–63]. Eppendorf® pO_2 histograph has been used over the past two decades to definitely establish the relevance of pO_2 measurements in radiation therapy [7], but its invasive nature led to its withdrawal from clinical practice. Among methods that are reporting actual pO_2 values, EPR offers the unique advantage of repeatable measurements from the same site over time after a single administration of an oxygen sensor [64]. Pioneering clinical EPR studies have used inks made of carbon black or charcoal particles [47, 48, 50, 64–66]. To pursue and extend the clinical EPR oximetry studies, there is a crucial

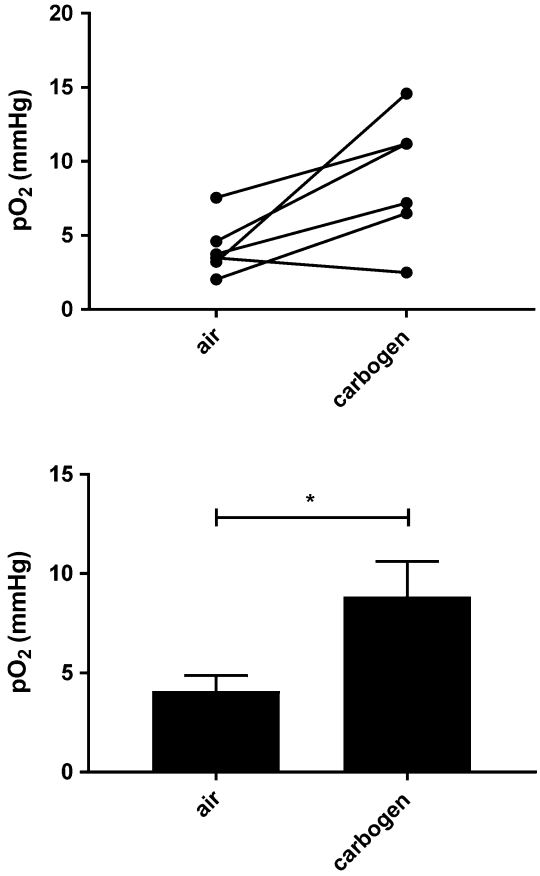

Fig. 7 pO_2 measurements ($n=6$) recorded in 9-L gliomas (in rats) after administration of Carbo-Rep®. Top: individual responses when switching from air to carbogen breathing. Bottom: mean pO_2 values ± standard error of mean (SEM) measured before and after 30 min carbogen breathing. *$P=0.0353$

need for the use of paramagnetic oxygen-sensitive probes that are recognized as medical devices. From our screening on carbon-based materials used in preoperative marking, our attention was drawn to Carbo-Rep®. We found that this

material presents a single-line EPR spectrum, with an LW highly sensitive to the oxygen environment (Fig. 1). The calibration curve (LW as a function of pO_2, Fig. 2) is comparable with other carbon-based oxygen-sensitive materials previously described [23, 24, 67, 68]. Interestingly, this charcoal formulation offers the maximal sensitivity in the range of physiological tissue oxygenation values (0–5% oxygen, or 0–38 mmHg) (Fig. 2). In addition, the accuracy of measurement was high, with an error estimated at ~0.5 mmHg at 1% oxygen. We also observed that variation in temperature may slightly affect the calibration (Fig. 2). As a consequence, for an accurate estimate of the pO_2, it is important to keep tissue temperature constant during measurements, especially when sedation or anesthesia is necessary. The injection of a small amount (75µl) of Carbo-Rep® suspension allowed recording an EPR signal using a Clin-EPR system (1-GHz EPR spectrometer) that could be further analyzed for LW estimation (Fig. 3). In muscles, the pO_2 measurements using EPR and Carbo-Rep® as the oxygen sensor were well within the range of physiological values found in other studies [27, 54, 55, 58]. As responsiveness stability is a critical issue when evaluating the performance of an oxygen sensor [53–55, 58], in vivo EPR measurements were repeated over a period of 6 months. Both baseline values and response to blood-flow restriction (Fig. 4) demonstrated Carbo-Rep® application allows for long-term oximetry. This feature is particularly interesting considering that clinical application of an EPR oxygen sensor has the potential for long-term monitoring of hypoxic status and oxygen changes in peripheral vascular diseases, wound healing [69, 70], and during the time course of radiation therapy [48, 71, 72]. To assess its potential application in the latter scenario, we administered Carbo-Rep® in a tumor model and evaluated the response to carbogen breathing, a treatment often used in an attempt to increase tumor oxygenation. We found that this charcoal preparation was capable of monitoring subtle changes in tumor oxygenation.

Conclusion

We identified a registered medical device that fulfills the requirements for oxygen measurements using EPR oximetry. This material, which is used clinically for preoperative localization of breast cancer, possesses EPR properties favorable for use as an oxygen sensor in future clinical EPR studies.

Acknowledgements The authors wish to thank Dr. Fabienne Danhier for performing the particle-size measurements.

Author contributions CMD, LBAT, PD: data acquisition, analysis, and interpretation; manuscript drafting; critical revision. BG: study conception and design; data analysis and interpretation; manuscript drafting; critical revision.

Funding The work was supported by the National Cancer Institute (NCI, USA) PO1CA190193, the Actions de Recherches Concertées ARC 14/19-058, and the Fonds Joseph Maisin. This research used the EPR facilities of the technological platform Nuclear and Electron Spin Technologies of the Louvain Drug Research Institute.

Compliance with ethical standards

Conflict of interest The authors declare that they have no conflict of interest.

Statement of human rights This article does not contain any studies with human participants performed by any of the authors

Statement on the welfare of animals All applicable international, national, and/or institutional guidelines for the care and use of animals were followed. All procedures performed in studies involving animals were in accordance with the ethical standards of the institution or practice at which the studies were conducted (authorization 2014/UCL/MD/026).

References

1. Springett R, Swartz HM (2007) Measurements of oxygen in vivo: overview and perspectives on methods to measure oxygen within cells and tissues. Antioxid Redox Signal 9:1295–1301
2. Vikram DS, Zweier JL, Kuppusamy P (2007) Methods for non-invasive imaging of tissue hypoxia. Antioxid Redox Signal 9:1745–1756
3. Colliez F, Gallez B, Jordan BF (2017) Assessing tumor oxygenation for predicting outcome in radiation oncology: a review of studies correlating tumor hypoxic status and outcome in the preclinical and clinical settings. Front Oncol 7:10
4. Bussink J, Kaanders JH, van der Kogel AJ (2003) Tumor hypoxia at the micro-regional level: clinical relevance and predictive value of exogenous and endogenous hypoxic cell markers. Radiother Oncol 67:3–15
5. Peeters SG, Zegers CM, Yaromina A, Van Elmpt W, Dubois L, Lambin P (2015) Current preclinical and clinical applications of hypoxia PET imaging using 2-nitroimidazoles. Q J Nucl Med Mol Imaging 59:39–57
6. Griffiths JR, Robinson SP (1999) The OxyLite: a fibre-optic oxygen sensor. Br J Radiol 72:627–630
7. Vaupel P, Höckel M, Mayer A (2007) Detection and characterization of tumor hypoxia using pO2 histography. Antioxid Redox Signal 9:1221–1235
8. Price JM, Robinson SP, Koh DM (2013) Imaging hypoxia in tumours with advanced MRI. Q J Nucl Med Mol Imaging 57:257–270
9. Howe FA, Robinson SP, McIntyre DJ, Stubbs M, Griffiths JR (2001) Issues in flow and oxygenation dependent contrast (FLOOD) imaging of tumours. NMR Biomed 14:497–506
10. Baudelet C, Gallez B (2002) How does blood oxygen level-dependent (BOLD) contrast correlate with oxygen partial pressure (pO_2) inside tumors? Magn Reson Med 48:980–986
11. Baudelet C, Gallez B (2004) Current issues in the utility of blood oxygen level dependent MRI for the assessment of modulations in tumor oxygenation. Curr Med Imaging Rev 1:229–243

12. O'Connor JP, Boult JK, Jamin Y, Babur M, Finegan KG, Williams KJ, Little RA, Jackson A, Parker GJ, Reynolds AR, Waterton JC, Robinson SP (2016) Oxygen-enhanced MRI accurately identifies, quantifies, and maps tumor hypoxia in preclinical cancer models. Cancer Res 76:787–795
13. Cao-Pham TT, Tran LB, Colliez F, Joudiou N, El Bachiri S, Grégoire V, Levêque P, Gallez B, Jordan BF (2016) Monitoring tumor response to carbogen breathing by oxygen-sensitive magnetic resonance parameters to predict the outcome of radiation therapy: a preclinical study. Int J Radiat Oncol Biol Phys 96:149–160
14. Kodibagkar VD, Wang X, Mason RP (2008) Physical principles of quantitative nuclear magnetic resonance oximetry. Front Biosci 13:1371–1384
15. Jordan BF, Cron GO, Gallez B (2009) Rapid monitoring of oxygenation by ^{19}F magnetic resonance imaging: simultaneous comparison with fluorescence quenching. Magn Reson Med 61:634–638
16. Swartz HM, Clarkson RB (1998) The measurement of oxygen in vivo using EPR techniques. Phys Med Biol 43:1957–1975
17. Gallez B, Baudelet C, Jordan BF (2004) Assessment of tumor oxygenation by electron paramagnetic resonance: principles and applications. NMR Biomed 17:240–262
18. Krishna MC, Matsumoto S, Yasui H, Saito K, Devasahayam N, Subramanian S, Mitchell JB (2012) Electron paramagnetic resonance imaging of tumor pO_2. Radiat Res 177:376–386
19. Ahmad R, Kuppusamy P (2010) Theory, instrumentation, and applications of electron paramagnetic resonance oximetry. Chem Rev 110:3212–3236
20. Epel B, Halpern HJ (2015) In vivo pO_2 imaging of tumors: oxymetry with very low-frequency electron paramagnetic resonance. Methods Enzymol 564:501–527
21. Liu KJ, Gast P, Moussavi M, Norby SW, Vahidi N, Walczak T, Wu M, Swartz HM (1993) Lithium phthalocyanine: a probe for electron paramagnetic resonance oximetry in viable biological systems. Proc Natl Acad Sci USA 90:5438–5442
22. Pandian RP, Parinandi NL, Ilangovan G, Zweier JL, Kuppusamy P (2003) Novel particulate spin probe for targeted determination of oxygen in cells and tissues. Free Radic Biol Med 35:1138–1148
23. Jordan BF, Baudelet C, Gallez B (1998) Carbon-centered radicals as oxygen sensors for in vivo electron paramagnetic resonance: screening for an optimal probe among commercially available charcoals. MAGMA 7:121–129
24. Lan M, Beghein N, Charlier N, Gallez B (2004) Carbon blacks as EPR sensors for localized measurements of tissue oxygenation. Magn Reson Med 51:1272–1278
25. Khan N, Mupparaju S, Hou H, Williams BB, Swartz HM (2012) Repeated assessment of orthotopic glioma pO_2 by multi-site EPR oximetry: a technique with the potential to guide therapeutic optimization by repeated measurements of oxygen. J Neurosci Methods 204:111–117
26. Ilangovan G, Liebgott T, Kutala VK, Petryakov S, Zweier JL, Kuppusamy P (2004) EPR oximetry in the beating heart: myocardial oxygen consumption rate as an index of postischemic recovery. Magn Reson Med 51:835–842
27. Jordan BF, Kimpalou JZ, Beghein N, Dessy C, Feron O, Gallez B (2004) Contribution of oxygenation to BOLD contrast in exercising muscle. Magn Reson Med 52:391–396
28. James PE, Miyake M, Swartz HM (1999) Simultaneous measurement of NO and pO_2 from tissue by in vivo EPR. Nitric Oxide 3:292–301
29. He G, Shankar RA, Chzhan M, Samouilov A, Kuppusamy P, Zweier JL (1999) Noninvasive measurement of anatomic structure and intraluminal oxygenation in the gastrointestinal tract of living mice with spatial and spectral EPR imaging. Proc Natl Acad Sci USA 96:4586–4591
30. James PE, Bacic G, Grinberg OY, Goda F, Dunn JF, Jackson SK, Swartz HM (1996) Endotoxin-induced changes in intrarenal pO_2, measured by in vivo electron paramagnetic resonance oximetry and magnetic resonance imaging. Free Radic Biol Med 21:25–34
31. Krzic M, Sentjurc M, Kristl J (2001) Improved skin oxygenation after benzyl nicotinate application in different carriers as measured by EPR oximetry in vivo. J Control Release 70:203–211
32. Van Eyck AS, Jordan BF, Gallez B, Heilier JF, Van Langendonckt A, Donnez J (2009) Electron paramagnetic resonance as a tool to evaluate human ovarian tissue reoxygenation after xenografting. Fertil Steril 92:374–381
33. Vériter S, Gianello P, Igarashi Y, Beaurin G, Ghyselinck A, Aouassar N, Jordan B, Gallez B, Dufrane D (2014) Improvement of subcutaneous bioartificial pancreas vascularization and function by coencapsulation of pig islets and mesenchymal stem cells in primates. Cell Transplant 23:1349–1364
34. Desmet CM, Lafosse A, Vériter S, Porporato PE, Sonveaux P, Dufrane D, Levêque P, Gallez B (2015) Application of electron paramagnetic resonance (EPR) oximetry to monitor oxygen in wounds in diabetic models. PLoS One 10:e0144914
35. Gallez B, Jordan BF, Baudelet C, Misson PD (1999) Pharmacological modifications of the partial pressure of oxygen in murine tumors: evaluation using in vivo EPR oximetry. Magn Reson Med 42:627–630
36. Jordan BF, Grégoire V, Demeure RJ, Sonveaux P, Feron O, O'Hara J, Vanhulle VP, Delzenne N, Gallez B (2002) Insulin increases the sensitivity of tumors to irradiation: involvement of an increase in tumor oxygenation mediated by a nitric oxide-dependent decrease of the tumor cells oxygen consumption. Cancer Res 62:3555–3561
37. Crokart N, Radermacher K, Jordan BF, Baudelet C, Cron GO, Grégoire V, Beghein N, Bouzin C, Feron O, Gallez B (2005) Tumor radiosensitization by antiinflammatory drugs: evidence for a new mechanism involving the oxygen effect. Cancer Res 65:7911–7916
38. Ansiaux R, Baudelet C, Jordan BF, Beghein N, Sonveaux P, De Wever J, Martinive P, Grégoire V, Feron O, Gallez B (2005) Thalidomide radiosensitizes tumors through early changes in the tumor microenvironment. Clin Cancer Res 11:743–750
39. Hou H, Khan N, Grinberg OY, Yu H, Grinberg SA, Lu S, Demidenko E, Steffen RP, Swartz HM (2007) The effects of Efaproxyn (efaproxiral) on subcutaneous RIF-1 tumor oxygenation and enhancement of radiotherapy-mediated inhibition of tumor growth in mice. Radiat Res 168:218–225
40. Crokart N, Jordan BF, Baudelet C, Cron GO, Hotton J, Radermacher K, Grégoire V, Beghein N, Martinive P, Bouzin C, Feron O, Gallez B (2007) Glucocorticoids modulate tumor radiation response through a decrease in tumor oxygen consumption. Clin Cancer Res 13:630–635
41. Diepart C, Karroum O, Magat J, Feron O, Verrax J, Calderon PB, Grégoire V, Leveque P, Stockis J, Dauguet N, Jordan BF, Gallez B (2012) Arsenic trioxide treatment decreases the oxygen consumption rate of tumor cells and radiosensitizes solid tumors. Cancer Res 72:482–490
42. O'Hara JA, Goda F, Liu KJ, Bacic G, Hoopes PJ, Swartz HM (1995) The pO_2 in a murine tumor after irradiation: an in vivo electron paramagnetic resonance oximetry study. Radiat Res 144:222–229
43. Crokart N, Jordan BF, Baudelet C, Ansiaux R, Sonveaux P, Grégoire V, Beghein N, DeWever J, Bouzin C, Feron O, Gallez B (2005) Early reoxygenation in tumors after irradiation: determining factors and consequences for radiotherapy regimens using daily multiple fractions. Int J Radiat Oncol Biol Phys 63:901–910
44. Cron GO, Beghein N, Crokart N, Chavée E, Bernard S, Vynckier S, Scalliet P, Gallez B (2005) Changes in the tumor microenvironment during low-dose-rate permanent seed implantation

iodine-125 brachytherapy. Int J Radiat Oncol Biol Phys 63:1245–1251
45. Fujii H, Sakata K, Katsumata Y, Sato R, Kinouchi M, Someya M, Masunaga S, Hareyama M, Swartz HM, Hirata H (2008) Tissue oxygenation in a murine SCC VII tumor after X-ray irradiation as determined by EPR spectroscopy. Radiother Oncol 86:354–360
46. Salikhov I, Walczak T, Lesniewski P, Khan N, Iwasaki A, Comi R, Buckey J, Swartz HM (2005) EPR spectrometer for clinical applications. Magn Reson Med 54:1317–1320
47. Swartz HM, Williams BB, Zaki BI, Hartford AC, Jarvis LA, Chen EY, Comi RJ, Ernstoff MS, Hou H, Khan N, Swarts SG, Flood AB, Kuppusamy P (2014) Clinical EPR: unique opportunities and some challenges. Acad Radiol 21:197–206
48. Swartz HM, Williams BB, Hou H, Khan N, Jarvis LA, Chen EY, Schaner PE, Ali A, Gallez B, Kuppusamy P, Flood AB (2016) Direct and repeated clinical measurements of pO_2 for enhancing cancer therapy and other applications. Adv Exp Med Biol 923:95–104
49. Gallez B, Mäder K (2000) Accurate and sensitive measurements of pO_2 in vivo using low frequency EPR spectroscopy: how to confer biocompatibility to the oxygen sensors. Free Radic Biol Med 29:1078–1084
50. Swartz HM, Liu KJ, Goda F, Walczak T (1994) India ink: a potential clinically applicable EPR oximetry probe. Magn Reson Med 31:229–232
51. Charlier N, Beghein N, Gallez B (2004) Development and evaluation of biocompatible inks for the local measurement of oxygen using in vivo EPR. NMR Biomed 17:303–310
52. Gallez B, Debuyst R, Liu KJ, Demeure R, Dejehet F, Swartz HM (1996) Development of biocompatible implants of fusinite for in vivo EPR oximetry. MAGMA 4:71–75
53. He J, Beghein N, Ceroke P, Clarkson RB, Swartz HM, Gallez B (2001) Development of biocompatible oxygen-permeable films holding paramagnetic carbon particles: evaluation of their performance and stability in EPR oximetry. Magn Reson Med 46:610–614
54. Dinguizli M, Jeumont S, Beghein N, He J, Walczak T, Lesniewski PN, Hou H, Grinberg OY, Sucheta A, Swartz HM, Gallez B (2006) Development and evaluation of biocompatible films of polytetrafluoroethylene polymers holding lithium phthalocyanine crystals for their use in EPR oximetry. Biosens Bioelectron 21:1015–1022
55. Dinguizli M, Beghein N, Gallez B (2008) Retrievable microinserts containing oxygen sensors for monitoring tissue oxygenation using EPR oximetry. Physiol Meas 29:1247–1254
56. Eteshola E, Pandian RP, Lee SC, Kuppusamy P (2009) Polymer coating of paramagnetic particulates for in vivo oxygen-sensing applications. Biomed Microdevices 11:379–387
57. Pandian RP, Meenakshisundaram G, Bratasz A, Eteshola E, Lee SC, Kuppusamy P (2010) An implantable teflon chip holding lithium naphthalocyanine microcrystals for secure, safe, and repeated measurements of pO_2 in tissues. Biomed Microdevices 12:381–387
58. Hou H, Khan N, Gohain S, Kuppusamy ML, Kuppusamy P (2018) Pre-clinical evaluation of OxyChip for long-term EPR oximetry. Biomed Microdevices 20:29
59. Baudelet C, Gallez B (2004) Effect of anesthesia on the signal intensity in tumors using BOLD-MRI: comparison with flow measurements by Laser Doppler flowmetry and oxygen measurements by luminescence-based probes. Magn Reson Imaging 22:905–912
60. Walsh JC, Lebedev A, Aten E, Madsen K, Marciano L, Kolb HC (2001) The clinical importance of assessing tumor hypoxia: relationship of tumor hypoxia to prognosis and therapeutic opportunities. Antioxid Redox Signal 21:1516–1554
61. Vaupel P, Kelleher DK, Höckel M (2001) Oxygen status of malignant tumors: pathogenesis of hypoxia and significance for tumor therapy. Semin Oncol 28:29–35
62. Horsman MR, Wouters BG, Joiner MC, Overgaard J (2009) The oxygen effect and fractionated radiotherapy. In: Joiner M, van der Kogel A (eds) Basic clinical radiobiology, 4th edn. H. Arnold, London, pp 207–216
63. Wouters BG, Korintzinsky M (2009) The tumor micro-environment and cellular hypoxia responses. In: Joiner M, van der Kogel A (eds) Basic clinical radiobiology, 4th edn. H. Arnold, London, pp 217–232
64. Khan N, Williams BB, Hou H, Li H, Swartz HM (2007) Repetitive tissue pO_2 measurements by electron paramagnetic resonance oximetry: current status and future potential for experimental and clinical studies. Antioxid Redox Signal 9:1169–1182
65. Swartz HM, Hou H, Khan N, Jarvis LA, Chen EY, Williams BB, Kuppusamy P (2014) Advances in probes and methods for clinical EPR oximetry. Adv Exp Med Biol 812:73–79
66. Flood AB, Wood VA, Swartz HM (2017) Using India ink as a sensor for oximetry: evidence of its safety as a medical device. Adv Exp Med Biol 977:297–312
67. Vahidi N, Clarkson RB, Liu KJ, Norby SW, Wu M, Swartz HM (1994) In vivo and in vitro EPR oximetry with fusinite: a new coal-derived, particulate EPR probe. Magn Reson Med 31:139–146
68. James PE, Grinberg OY, Goda F, Panz T, O'Hara JA, Swartz HM (1997) Gloxy: an oxygen-sensitive coal for accurate measurement of low oxygen tensions in biological systems. Magn Reson Med 38:48–58
69. Swartz HM, Khan N, Buckey J, Comi R, Gould L, Grinberg O, Hartford A, Hopf H, Hou H, Hug E, Iwasaki A, Lesniewski P, Salikhov I, Walczak T (2004) Clinical applications of EPR: overview and perspectives. NMR Biomed 17:335–351
70. Desmet CM, Préat V, Gallez B (2018) Nanomedicines and gene therapy for the delivery of growth factors to improve perfusion and oxygenation in wound healing. Adv Drug Deliv Rev 129:262–284
71. Matsuo M, Matsumoto S, Mitchell JB, Krishna MC, Camphausen K (2014) Magnetic resonance imaging of the tumor microenvironment in radiotherapy: perfusion, hypoxia, and metabolism. Semin Radiat Oncol 24:210–217
72. Epel B, Maggio M, Pelizzari C, Halpern HJ (2017) Electron paramagnetic resonance pO_2 image tumor oxygen-guided radiation therapy optimization. Adv Exp Med Biol 977:287–296